9
Computed Tomography Imaging for Tumor Ablation

Thierry de Baère

Computed tomography (CT) affords the best visualization of all organs in the body, simultaneously depicting air, soft tissue, and bones on the same scan. This ability makes CT an ideal imaging modality for tissue ablation, as it enables the physician to target any type of organ accurately and to avoid inadvertently puncturing others along the needle path. However, in the past, as the duration of image acquisition and reconstruction was long with CT, this time-consuming aspect appeared inconvenient for tissue ablation. Recent improvements in computerized data management have transformed CT into almost a real-time imaging technique, and even more recently, the advent of multislice CT has made imaging of a volume in a single acquisition feasible, thereby improving the scope of CT guidance for tissue ablation. CT can now be used throughout tissue ablation for guidance, monitoring, and follow-up.

Image guidance is critical when ablating a tumor, because accurate positioning of the ablation instrument in the targeted tumor is a key factor for treatment efficacy. Moreover, accurate guidance avoids nontargeted structures or organs located close to or in the path of the tumor.

Image monitoring is also important. Ablation should be tailored to the tumor target volume to avoid incomplete treatment, recurrence, and the need for re-treatment. Injury to neighboring tissue and collateral damage also can be evaluated in real time.

Follow-up imaging is mandatory after tumor ablation because monitoring techniques and current ablation systems are unable to confirm complete tumor eradication at the time of treatment. The treated organ, therefore, requires follow-up imaging to ascertain whether ablation of the targeted tumor was efficient, as well as to detect new tumors and treatment complications.

Image Guidance

Indications

The first step in the ablation procedure is to guide the ablation instrument (the probe, the needle, the fiber, the electrode) toward the targeted tumor. Imaging used for guidance should clearly depict the ablation instrument and the targeted tumor, so that the instrument is positioned accurately within the tumor. Computed tomography is mandatory for guidance when it is the only technique capable of imaging the targeted tumor. Such is the case for most lung and bone tumors, given that fluoroscopic guidance is not accurate enough, and that interventional magnetic resonance (MR) is far from commonplace today. Such is also the case for some soft organ tumors that are not well defined by ultrasound (US). Computed tomography can be useful when the tumor is depicted by US, but is virtually inaccessible for puncture with US on account of the location, or because gas or bones obstruct the imaging window or needle tract. For example, tumors that are seated high in the liver are sometimes inacces-

E. vanSonnenberg et al., *Tumor Ablation*

sible to puncture under US, whereas CT guidance allows access via the transthoracic route, which is impossible with US guidance due to air in the lung that obstructs the imaging window. Computed tomography is also preferred when a safe pathway to the targeted tumor cannot be imaged with US, for example, when a hollow organ containing air is very close. Finally, combining CT and US guidance sometimes can be useful. Computed tomography can be used to guide the ablation instrument toward the targeted organ along a safe tract that cannot be easily depicted with US, and once the organ has been reached, US can then be used to guide the instrument in real time into an ill-defined tumor on CT.

When tumor visualization and accessibility for puncture are equivalent under both US and CT guidance, the technique of choice is that preferred by the operator or according to the availability of the equipment. In clinical practice today, most liver tumors are treated under US guidance because this technique is widely available, the cost is low, angulation possibilities are virtually limitless, and real-time guidance is achievable. Today, with the advent of almost real-time CT, often called CT fluoroscopy (fluoro-CT), the time required for needle insertion during ablation is short, thus overcoming the previous drawback with CT. A comparative study on a phantom demonstrated no significant differences between US and fluoro-CT in the time needed to guide a biopsy; helical CT guidance was threefold longer (1).

Technique

Some technical requirements need to be emphasized. The gantry must be large enough to allow the passage of the instrument that has been partially inserted in the patient. As some handles on the instruments are quite long, a handle-less guiding trocar needle or a flexible device may facilitate placement in the tumor. For practical and sterility reasons, a TV screen is mandatory inside the CT room. It is also useful to have a footswitch to use to direct and release the table, and to be able to perform CT acquisition inside the room. To minimize radiation to the patient and to the physician, the dose and time must be limited. The quality of the image needed for guidance is not the same as that needed for diagnostic purposes, and usually is not as good.

Scanning time should be as short as possible for image reconstruction. Consequently, almost real-time CT imaging, or fluoro-CT, is now preferred. Continuous fluoro-CT with systems able to produce at least eight images per second with a reconstruction time of less than 0.2 second allows almost real-time guidance. This has been demonstrated to shorten the duration of the puncture procedure, and to improve the accuracy of tumor targeting, demonstrated by an increase in the sensitivity and the negative predictive value when used for biopsy (2).

If imaging time is maintained at a minimum, and certain precautions such as milliampere reduction for scans to evaluate needle position, fluoro-CT does not increase the dose to the patient or the physician (3). However, one of the drawbacks of real-time fluoro-CT is that the needle is handled by the physician while x-rays are being delivered, and this increases the radiation received by the physician's hands that are in, or close to, the imaging field. Special needle holders have been designed so that the physician can guide the needle while keeping his/her hands away from the x-ray beam (4,5). To further minimize radiation delivered to the patient and the physician, the "quick-check" technique can be used. This technique uses brief single-section fluoro-CT imaging that is repeated whenever the needle is advanced, but unlike real-time fluoro-CT, the needle is advanced without real-time imaging. The quick-check technique is accurate and rapid for guiding the needle to the target (6). In practice, the quick-check technique is adequate for the majority of cases. Continuous fluoro-CT probably should be reserved for difficult cases, for example, in moving structures, or when the access for the target is narrow, or finally for the actual puncture when the instrument is penetrating the targeted tumor.

Multislice CT is even more user friendly for puncturing under CT guidance, as it offers one or two center rows to image the needle course, and two lateral ones to ensure that the instru-

ment does not overstep the track in the upper or lower imaging planes. The most recent multislice CT unit with up to 16 rows provides rapid three-dimensional (3D) volumetric imaging to such an extent that it may be possible in the near future to guide the needle in all planes with the help of real-time reconstruction. However, this type of software is not capable of providing oblique multiplanar imaging in real-time as yet. This is why, even today, a perpendicular approach is always preferred when possible, because it is the simplest. If an angled approach is used, it allows the entire puncture tract and needle to be imaged in one slice (7).

In practice, the procedure for inserting the ablation instrument begins with a detailed CT examination of the region. The patient is placed in the most favorable position for access to the entry point. Treatment of a limb tumor may require a different degree of rotation. Securing the limb with tape or straps can be useful during treatment of bone tumors, because the force required for drilling can cause extremity movement that can be bothersome on subsequent CT scans. Next, the level of the targeted slice is highlighted with a laser marker light, and the entry point is marked on the skin. A metallic marker can be used to delineate the entry point precisely. The anticipated angle of the path and depth of the target are determined according to this entry point using the electronic calipers on the CT console.

Once these parameters have been defined, it is often useful to stick a short, small-caliber needle in this entry point that can be used for local anesthesia if needed. This needle confirms that the entry point and tract angulation are accurate on the subsequent CT scan, before insertion of the ablation instrument using the tandem technique. Then, while the clinician is advancing the instrument, CT imaging can be obtained at regular intervals to verify the depth and direction of the incoming instrument, and this depends on the rapidity of image acquisition and reconstruction. Real-time fluoro-CT or quick-check imaging can be used, as discussed above. A distal shadow due to a partial-volume effect allows the physician to distinguish the tip of the instrument, but one should always image a slice above and another below the tool to ensure that the tip is not overstepping the reference slice.

With conventional CT guidance, only tumors visualized without injection of contrast medium were punctured, because the time necessary to perform the puncture was longer than the duration of enhancement. Nowadays, with fluoro-CT, a tumor can be punctured during transient enhancement, as described in the literature for tumors enhancing from 50 to 130 seconds (8,9). The target lesion should be in the scan plane to do so. This scan plane and delayed imaging should be determined according to temporal measurement of delay times, based on the previous diagnostic CT examination. The physician should be ready, standing at the side of the patient clothed in a sterile garment in front of the gantry, poised for the puncture.

When the puncture cannot be performed within gantry angulation possibilities, it will be less accurate and more time-consuming. In the past, the only alternative was to use the triangulation technique in such situations. Today, guidance with a laser goniometer (10) or electromagnetic virtual targeting systems (11) can be extremely helpful as they heighten accuracy and shorten the duration of the procedure and the number of needle passes. However, the remaining disadvantage of these out-of-plane techniques is the nonvisualization of the complete needle on a single image. Electromagnetic targeting systems are composed of a computer that is first loaded with a set of reference CT scans obtained immediately before puncturing the tumor, and the patient is maintained immobile thereafter. This set of CT scans encompasses the target and the entry point when an out-of-plane puncture is needed, or provides a single reference slice when an in-plane puncture is to be performed. The target and the entry point are then marked with calipers on the screen of the targeting system. Before actually inserting the needle, a virtual needle path can be visualized on the set of CT scans, and multiplanar reconstruction can be performed in any direction and angulation. Once this viewing has demonstrated that no vital structures would be violated, the puncture can be performed following the direction indicated on the screen of the guiding system. During the puncture, an

electromagnetic sensor placed on the proximal needle, close to the needle hub or instrument handle, allows (with the help of algorithms similar to those used in global positioning systems) accurate localization of the needle tip in real time, as well as the route chosen by the physician, both of which are superimposed over the reference set of previously loaded images (Fig. 9.1). The electromagnetic targeting system has a built-in respiratory phase monitoring system that allows the needle to be inserted during the same phase of the respiratory cycle as that during which reference images were acquired. As the position of the needle tip and its future route and position are a "straight projection" of the direction of the proximal part of the needle, great care should be taken not to bend the needle, as this will lead to incorrect projection of the position of needle tip and future path. Using a small-gauge needle with a bevel can be problematic, since the needle tract may become curved. Rotating the needle while advancing it has been described to minimize possible curving and deviation.

The laser goniometer is a laser light unit that can be either attached to the gantry or be separate from it. Angulate coordinates, determined on the CT unit from previously acquired slices, are calculated. Then the laser beam is angulated according to these coordinates, and focused on the entry point on the patient's skin. The direction of the needle is kept within the laser beam, demonstrating the desired angle while advancing the needle for the puncture. The greatest contribution of such a system occurs when performing double angulation punctures within the limits of gantry angulation (10,12).

As thermal ablation instruments are relatively large in caliber, the best option is to access the target organ without traversing any other structure. When the window for safe access to the target organ is quite narrow, or even virtual, the physician can inject a large volume of saline to widen the path artificially by enlarging the anatomic space between two organs. This technique has been reported for biopsy in the mediastinum (13,14), the retroperitoneum (15), and the pelvis (16). For this technique, first, a small (often 22 gauge), caliber needle is inserted as deeply as possible in the narrow tract chosen for insertion. Then, saline is manually injected slowly to enlarge the tract and move the untargeted organ away. The needle is then advanced further and the injection is repeated until a large-enough area is created for insertion of the ablation instrument. Usually 10 to 30 mL of saline are used, but up to 60 mL may be required.

In high-seated liver tumors that are inaccessible under US, access using CT often is diffi-

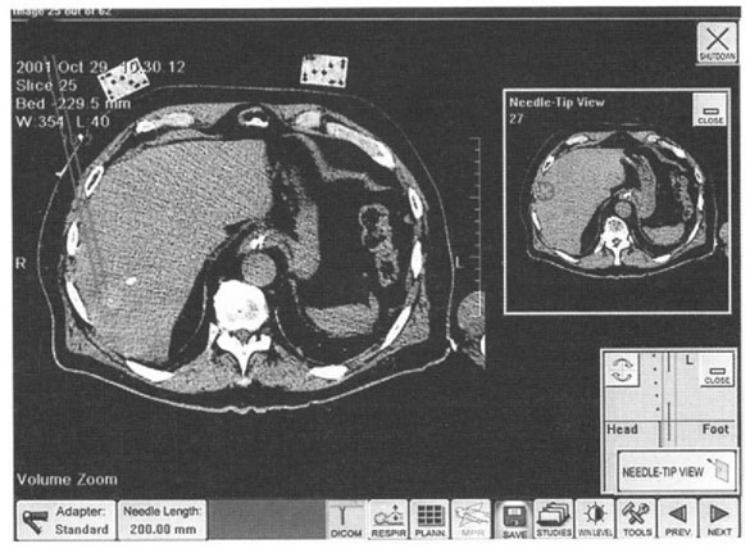

FIGURE 9.1. View of the screen of an electromagnetic targeting system. The circle on the right frame represents the location of the needle tip. The parallel lines on the left frame represent the future needle path; the distance to the target is also shown. Note the two respiratory sensors on the anterior abdominal wall used to monitor the respiratory cycle. (Courtesy of Dr. Afshin Gangi.)

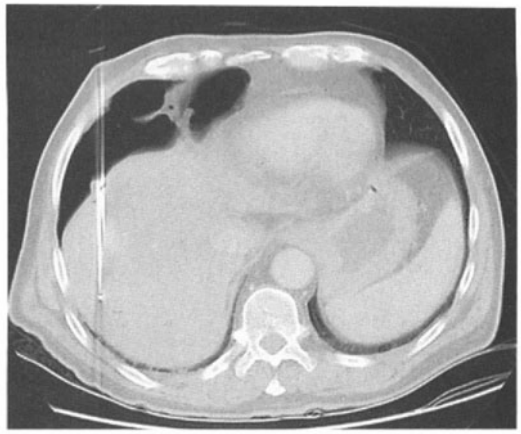

FIGURE 9.2. Computed tomography (CT) scan depicts insertion of a cool-tip cluster radiofrequency (RF) needle in a very high-seated segment VII liver metastasis via an air-filled right pleural cavity. The large right pneumothorax has been induced to avoid piercing the lung. This pneumothorax will be expelled after transpleurodiaphragmatic RF ablation.

cult or impossible via a transhepatic route as well. Transpulmonary access has been described for ethanol injection in hepatocellular carcinomas, but pneumothoraces occur in 30% of the cases and require a chest tube in 7% (17). Even if some ablative techniques, such as radiofrequency (RF), are used in the lung, in our opinion it is safer to try and avoid collateral lung damage. When transpleural access is needed, we first induce a pneumothorax to retract the lung toward its hilum. A path for the ablation instruments is thus created in a pleural cavity that is transiently devoid of lung parenchyma and filled with iatrogenic air (Fig. 9.2). The pneumothorax is induced with an epidural needle by maintaining positive pressure on the piston of an air-filled syringe during the puncture in a similar manner to an epidural injection. When the needle tip reaches the pleural space, the decrease in resistance will allow a few milliliters of air to be injected. CT is then used to check that the needle is positioned correctly and that air has been injected in the right location. Then, the amount of air needed to move the lung away from the future needle path is aspirated through a filter, and manually injected into the pleural cavity. Usually, 100 to 400 mL of air are enough to clear the lung from the needle path. Finally, the lung is separated from the diaphragm; then the liver can be accessed through the air-filled pleural space while avoiding injury to the lung, and reproducing, in a manner akin to the surgical transpleurodiaphragmatic access described by surgeons, an efficient way of treating tumors of the dome of the liver (18). At the end of the ablation procedure, the needle is exchanged over a 0.035-inch wire for a 5-French side-hole catheter to remove air from the pneumothorax, and to expel it through a three-way stopcock.

Treating tumors in proximity to organs that are sensitive to heat or cold can cause collateral damage to these organs. Such complications have been reported to occur in the colon, stomach, and gallbladder when treating liver tumors, and to nerve roots when bone tumors are treated with RF. Clearly, the simplest way to avoid such collateral damage is not to treat tumors that are less than 1 cm from sensitive organs. Another option is to refer the patient for a preoperative or laparoscopic ablation procedure during which the untargeted organ will be manually moved away from the targeted organ. Finally, when a percutaneous approach is required, one can try to move the tumor away from the untargeted organ. A thin needle can be inserted in the narrow or virtual space between the two organs for this purpose, and then a few milliliters of air or saline (a test amount) are injected. Once injection in the targeted space has been confirmed, a larger amount of air/saline can be used. This technique can be used, for example, in the peritoneum in an attempt to widen the space between a peripheral liver tumor and a sensitive organ such as the colon or stomach (Fig. 9.3). In this setting, CT imaging provides a unique and accurate view of any structure, as well as the injected air or saline.

Positioning of the ablation instrument in relation to the tumor under CT guidance is akin to placing the needle in a biopsy procedure. However, a major difference between ablation and biopsy is that sampling in the latter can be performed practically anywhere in the tumor

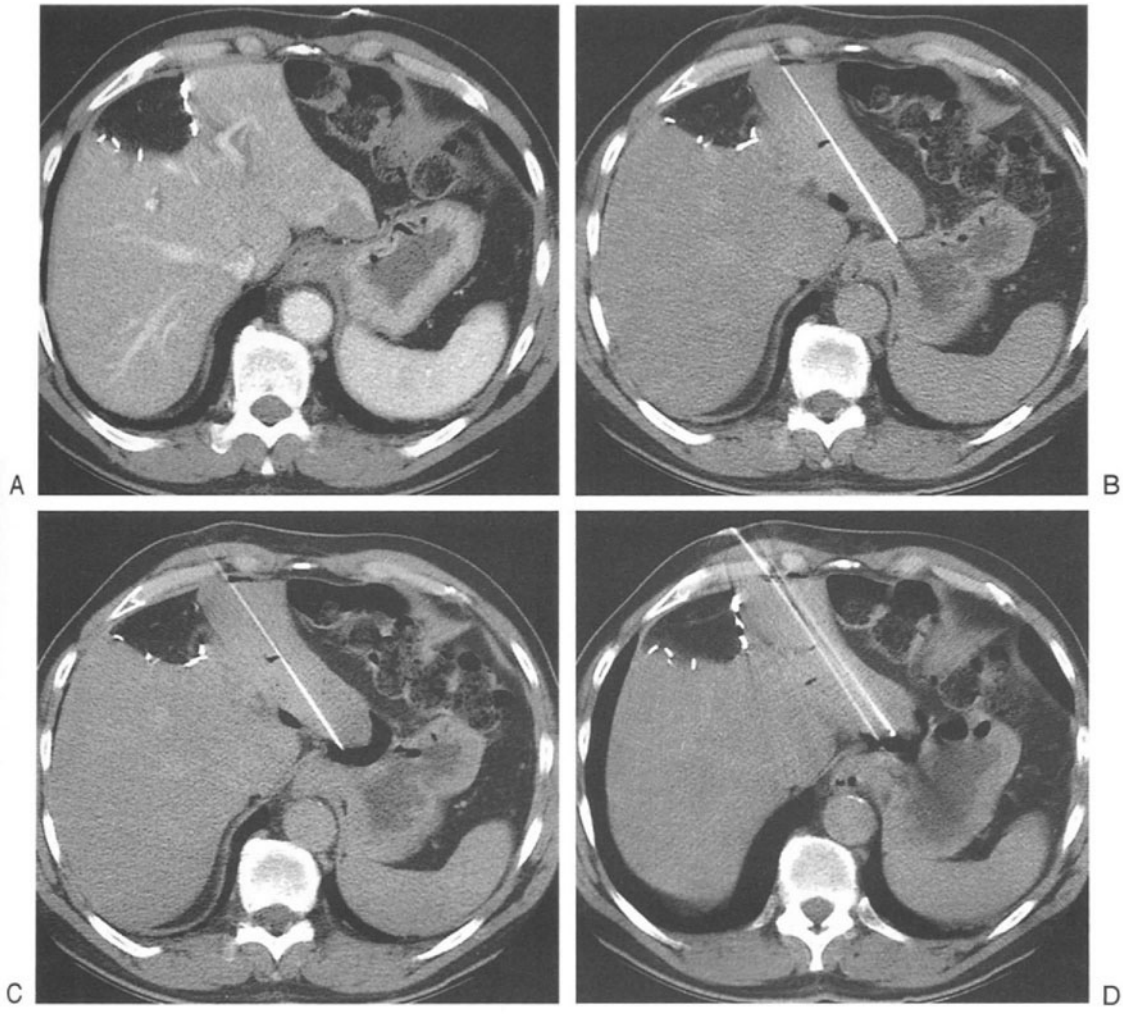

FIGURE 9.3. (A) A CT scan shows a segment I liver metastasis abutting on the gastric wall, which developed after liver surgery. (B) The tip of a 22-gauge Chiba needle, inserted via a transhepatic route under CT guidance, is located in the narrow space between the stomach and segment I of the liver. (C) Ten milliliters of air have been manually injected through the needle, allowing the gastric wall to be moved away from the subcapsular metastasis in segment I. (D) A cool-tip RF needle is placed in the metastasis in segment I and thermal ablation can be performed without collateral damage to the stomach. (Courtesy of Dr. Philippe Brunner.)

provided a necrotic center, if present, is avoided. During ablation therapy, the active tip of the probe must be positioned in a precise location inside the targeted tumor. Most of the time the ablation site should be in the center of the tumor so that the entire lesion is destroyed, along with a rim of healthy tissue. Entering the tumor only once without completely traversing it with the tip of the needle is of paramount importance. Multiple punctures can lead to tumor cell spillage and seeding. This is also pertinent when expandable multiple-array needles are used for RF ablation; being in the right location is critical to avoid repeated deployment of the hook-shaped inner electrodes, as this is likely to promote tumor seeding.

Accurate positioning of the ablation instrument in relation to the tumor usually is evalu-

ated on axial images without contrast injection. In some instances, contrast injection can be useful, particularly when the contrast between the tumor and the surrounding liver is low. Thin control scans should be used, because although thick scans make it easier to visualize the lesion, they are less accurate to judge the probe position in relation to the target. Moreover, it has been demonstrated that the use of multiplanar reformation in the coronal and sagittal planes statistically improves the accuracy of instrument placement. In 44% of cases, instrument repositioning was required under imaging guidance in the axial plane (19).

When tumors are larger than the volume of ablated tissue that can be obtained in one application, overlapping ablation is needed to attempt to destroy the tumor completely. When such overlapping ablations are needed, CT probably has an edge over ultrasound for monitoring. The overriding advantage is that the probe position is easier to visualize with CT than with US after changes caused by previous ablations. Indeed, the slight decrease in Hounsfield units (HU) exhibited by the thermal lesions on CT (see Image Monitoring, below) does not impede subsequent instrument placement at all, and can even be useful for guidance. The second advantage is that CT multiplanar reconstruction can probably help to position the probes equidistantly in any direction, and that would be ideal placement. In contrast, postablation US imaging demonstrates either hyperechoic or hypoechoic tissue changes, but always with posterior shadowing that impedes visualization of the tumor or needle. Subsequent probe placement is difficult, and inevitably inaccurate, even if the basic recommendation to treat the deepest part of the tumor first is followed. Whatever the guidance system used, it should be borne in mind that if overlapping deliveries are to be performed, six deliveries will only increase the diameter of the thermal lesion by 25% (20), and the efficacy of local ablation decreases rapidly when the size of the target increases (21).

Liver tumors should be punctured via the shortest route possible, avoiding large vessels, and, of course, the liver hilum, as well as the gallbladder. However, when tumors are subcapsular, it is always preferable to first traverse healthy liver parenchyma to avoid bleeding and tract seeding. Indeed, tumor seeding along the needle tract has been reported to occur particularly after treatment of subcapsular hepatocellular carcinomas. Treating the tract with cauterization is a potential option to try to minimize such seeding and bleeding. *A word of warning*: Treatment of the liver capsule is always painful and thus requires deep sedation.

Computed tomography guidance is often used for bone tumors because of the high quality of visualization it provides. Planning an entry point perpendicular to the bone surface helps avoid slippage and potential damage to other organs. Drilling the cortical bone is often required to reach a deep-seated lesion. For example, a safe anatomic entrance is sometimes via the normal cortex on the opposite side. After drilling, a sheath or a guiding needle can be useful to exchange the drill for the ablation instrument. It is therefore advisable to use a drill needle that is at least one gauge larger than the ablation tool. If the external metallic sheath of the drill system is used to guide the ablative tool for RF or microwave ablation, one should retract the sheath a few centimeters before power deposition to avoid contact between the active part of the probe and the metallic sheath; this contact could cause burns along the track and must be avoided (Fig. 9.4). A plastic sheath is preferred for cryotherapy to avoid freezing of the track.

Osteoid osteoma is a good indication for ablation. Laser and RF have both been reported to be effective to treat osteoid osteomas (22–24). More sophisticated and larger caliber devices such as cooled or expandable multiple-array needles are not required for osteoid osteomas, as the target is small and a single bare laser fiber or a single RF needle is sufficient. On the other hand, in the case of large osteolytic bone tumors, good results have been demonstrated with the expandable multiple-array needle probe for treatment of pain in cases refractory to standard management with analgesics and radiation therapy (25). When used to manage pain, this particular needle is usually chosen to target the margin of

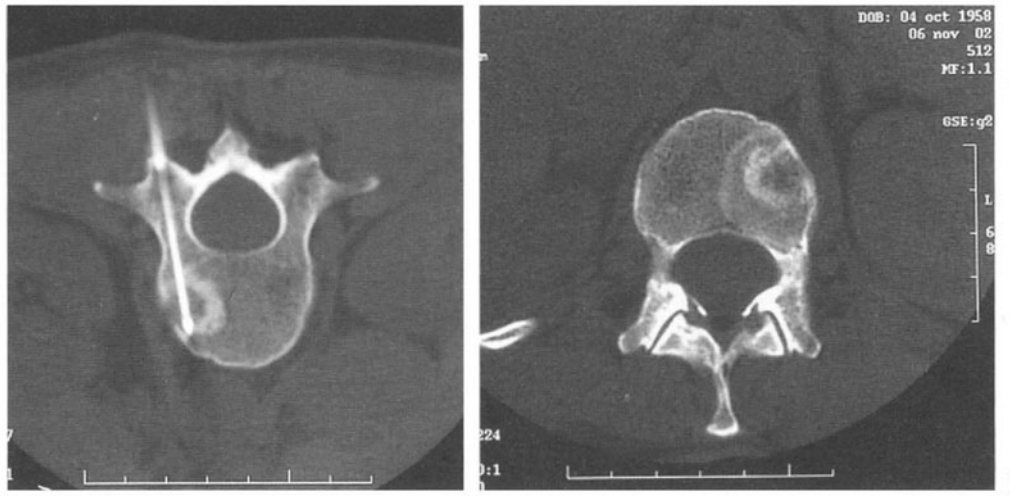

FIGURE 9.4. (A) A CT scan of second lumbar vertebral body lytic metastasis from breast cancer, which has been accessed via a transpedicular approach. A single cool-tip RF needle has been inserted through the metallic sheath of the drill needle. A few centimeters of the sheath have been retracted, up to the level of the cortical bones, to avoid contact between the metallic sheath and noninsulated distal part of the needle. (B) Two months after RF delivery, CT scan shows a rim of hyperattenuating tissue, seemingly delimiting the external borders of the ablated area.

metastases that involve bones with the objective of treating the soft tissue–bone interface, especially when the entire tumor volume cannot be destroyed because the metastases are large. It is straightforward to achieve such targeting under CT guidance, and is important because sensory nerve fibers involving the bone periosteum and cortex can be destroyed to inhibit pain transmission. The expandable multiple-array RF needle is difficult to deploy when dealing with large osteoblastic bone tumors. Nonexpandable probes are preferred in this situation.

When treating lung tumors, the needle path should traverse the shortest length of aerated lung parenchyma, avoiding fissures and minimizing the number of passes through the pleural surfaces. Transgression of fissures and pleural surfaces increases the incidences of pneumothoraces (26). Furthermore, trying to insert a needle as perpendicular as possible to the pleura also appears to be important in averting the risk of pneumothorax (27). Whatever the ablation technique used, it is recommended that only one lung be treated at a time to avoid life-threatening complications that can occur in cases of bilateral adverse events such as massive hemorrhage (28) or pneumothorax. Notwithstanding, several tumors can be treated on one side during the same session. Using an expandable needle for lung RF ablation may be an advantage, as this type of needle will not slip out of the tumor in case of a massive pneumothorax that can push the target tumor away from the needle. The physician should be ready to insert a chest tube if a significant pneumothorax occurs. Computed tomography imaging is useful for chest tube placement if a postablation pneumothorax occurs while the patient is still on the CT table. We usually try to manually expel the pneumothorax by inserting a 5-French side-hole catheter in the air-filled pleural cavity under CT guidance. This catheter is connected to a 50-mL syringe via a three-way stopcock; air is drawn from the pneumothorax into the syringe and then expelled. Larger caliber chest tubes are used only in cases of recurrent pneumothorax.

Image Monitoring

As no imaging technique is capable of confirming cell death with 100% accuracy, there is no way of knowing whether the tumor has been completely destroyed at the time of treatment. Image monitoring of the ablation procedure rarely examines the extent of treatment directly. Only MR thermometry directly evaluates the extent of heat or cold. All the other imaging techniques simply image changes that are indirect consequences of treatment. These modifications do not correspond exactly to the extent of the ablated volume, nor to certain cell death within the volume. In the liver, for example, US monitoring depicts a hyperechoic area induced by the formation of gas after RF, laser, or microwave ablation; US demonstrates a hypoechoic iceball after cryotherapy, and hyperechoic changes after alcohol injection. The consequences of treatment depicted by MR imaging are areas of hypointense signal following cryotherapy and RF, and/or devascularized tissue that any ablative technique can produce.

Most of the data and experience with CT monitoring of tissue ablation are related to RF ablation. RF ablation in the liver was well described in an animal study by Cha et al (29), in which CT was performed immediately and 2 and 8 minutes after treatment. Unenhanced CT scans 2 minutes after RF showed a 14-HU decrease in ablated tissue compared to healthy liver, and this difference increased to 22 HU at 8 minutes. After cryotherapy, frozen tissue also was described as a well-demarcated region of lower attenuation than normal liver (30).

After hyperthermia or cryoablation, the postablation hypoattenuating area on CT often contains several small gas bubbles of various sizes that are irregularly distributed in the ablated tissue. After injection of contrast medium, the differences between RF-ablated tissue and healthy liver increase to 55 HU, with improved conspicuity and edge detection. CT was found to correlate better than US with the real volume of ablated liver tissue measured at pathologic examination (29,31); the peripheral rim of enhancement that corresponds to an inflammatory reaction is not taken into account for the measurement of ablated tissue. Ultrasound slightly underestimated the true size of ablated tissue. Better correlation with the pathologic study also has been reported for CT monitoring versus intraoperative US in the kidney (32).

As enhanced CT provides a more clear-cut delineation of the ablated area than unenhanced CT, enhanced CT is performed at the end of the treatment to try to best determine the extent of coagulation. The goal of ablation is to obtain an unenhanced area that is at least as large as the tumor, and ideally a few millimeters larger. Of course, if the targeted tumor exhibits high enhancement before ablation, disappearance of this enhancement must be achieved. If tumor enhancement persists, CT allows retargeting of residual foci during the same treatment session. As the amount of contrast medium that can be injected is limited and enhancement is less intense after subsequent injections, enhanced imaging cannot be repeated at will. The use of contrast medium at CT optimally is left for the final evaluation.

During chemical ablation, CT is able to image the spatial diffusion of the injected liquid. Alcohol is slightly hypoattenuating, but any toxic liquid or gel can be transformed into a hyperattenuating substance by adding contrast medium to the therapeutic compound, as reported for alcohol (33,34) or chemotherapeutic drugs (35). Once again, although imaging is capable of depicting the diffusion of the toxic agent, it cannot predict the efficacy of the treatment. Here again, injection of contrast medium can help to evaluate the extent of coagulation necrosis by imaging the unenhanced area; conversely, an area of the tumor with persistent enhancement can be subsequently targeted for retreatment, as reported for alcohol therapy of hepatocellular carcinomas (HCCs) (4).

Computed tomography monitoring of thermal ablation in bone or kidney tumors delineates roughly the same features as described previously in the liver. The formation of gas bubbles at irregularly distributed points within the ablated lesion is common. If the tumor is initially highly enhanced, this enhancement disappears if treatment is efficient; otherwise there is a small decrease in density.

In the lung, RF ablation causes lung tissue to became more dense in the ablated area (Fig. 9.5). This is akin to alveolar consolidation, and is often very faint during the course of treatment. It becomes more intense and slightly more extensive during the following hours and days (see Follow-Up Imaging, below). Although it is unclear whether these CT imaging changes

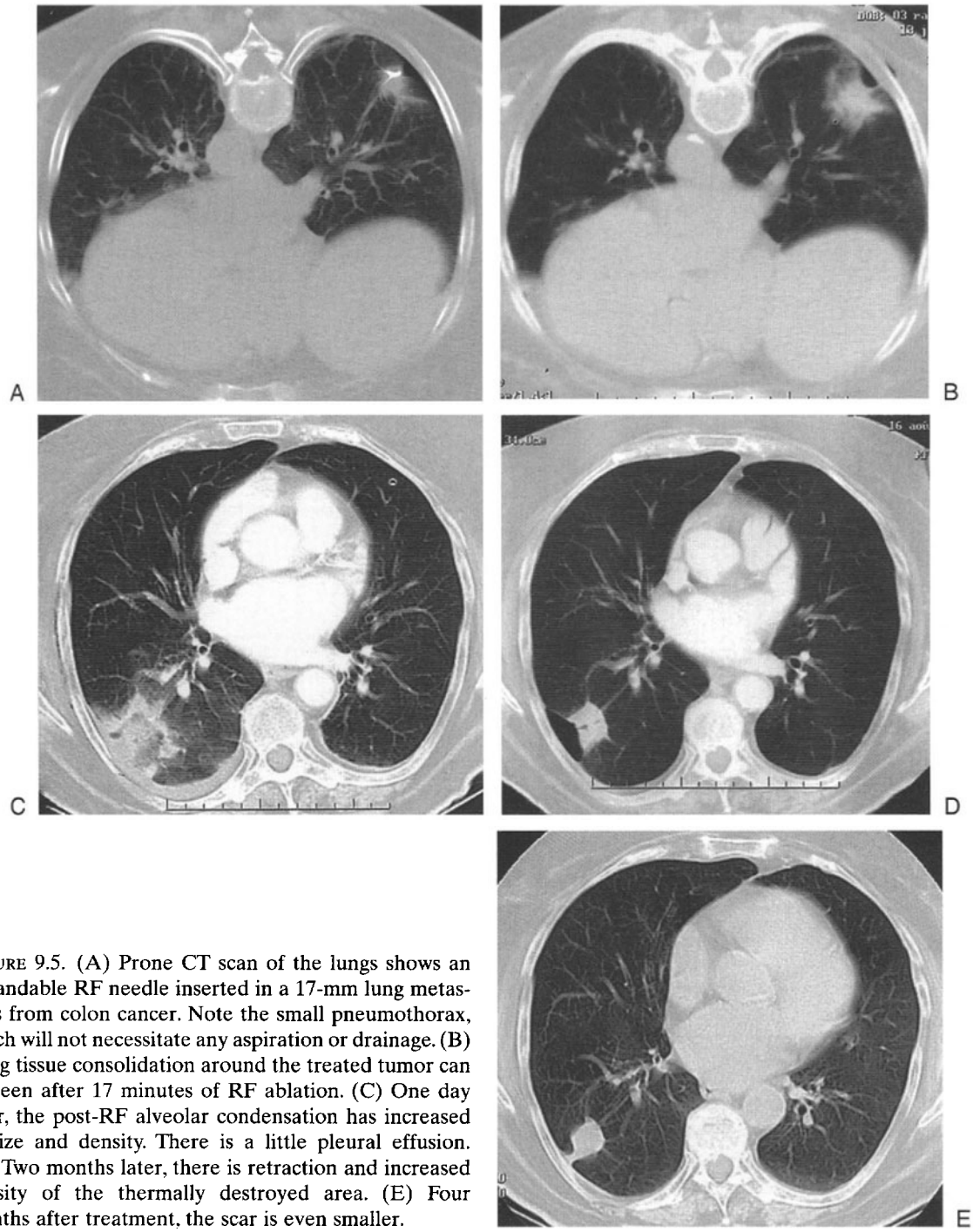

FIGURE 9.5. (A) Prone CT scan of the lungs shows an expandable RF needle inserted in a 17-mm lung metastasis from colon cancer. Note the small pneumothorax, which will not necessitate any aspiration or drainage. (B) Lung tissue consolidation around the treated tumor can be seen after 17 minutes of RF ablation. (C) One day later, the post-RF alveolar condensation has increased in size and density. There is a little pleural effusion. (D) Two months later, there is retraction and increased density of the thermally destroyed area. (E) Four months after treatment, the scar is even smaller.

really represent coagulation necrosis, this area of density is helpful when attempts are made to shape the thermal lesion so that it is equivalent to the tumor size.

Follow-Up Imaging

As stated earlier, there is no way of affirming that a tumor has been completely ablated during the procedure itself. Consequently, follow-up imaging is crucial to determine treatment efficiency, or, on the contrary, local failure of ablation. When failure occurs, follow-up imaging is used to image the location of residual tumor accurately for further ablative therapy. As the tumor size is a critical factor in the efficacy of ablation, it is important that regrowth be unveiled as early as possible to optimize retreatment of small lesions. Thus, follow-up imaging should be performed at regular intervals and over a long period of time, because incomplete ablation often leaves small undetectable tumor foci that will be visible on delayed imaging only when the residual cells have grown to form a larger tumor (Fig. 9.6).

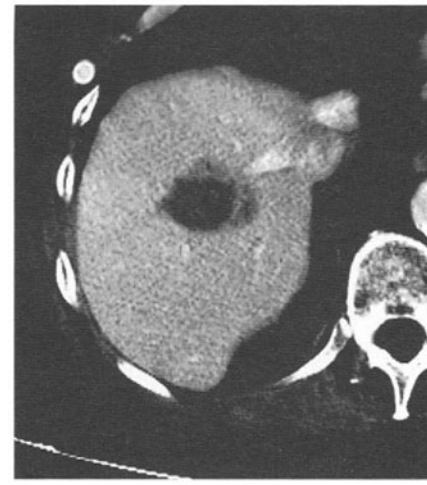

FIGURE 9.6. Four months after RF ablation of a metastasis from colon cancer, CT scan shows a hypoattenuating unenhanced round area corresponding to ablated tissue. The heterogeneously enhanced curviform area at the anteromedial border of the scar, in contact with the middle hepatic vein, has appeared since the previous CT scan performed 2 months earlier. This is tumor regrowth from residual unablated foci. This incomplete ablation has probably been promoted by heat sink induced by the neighboring large hepatic vein.

As the aim of ablation is to generate an area of necrosis, the diameter of which is larger or at least equivalent to that of the tumor. Ideally, the destroyed tissue or "scar" should be larger than the treated lesion, encompassing the tumor and safety margins. If treatment is successful, this scar will decrease in size, albeit slowly. Indeed, in our experience with mostly colon cancer metastases in the liver, 66% of successfully treated tumors decreased in size during 12 months of imaging follow-up. The decrease in the product of the two largest dimensions of the scar attained a mean of 15% (range 10–30%) at 6 months, and 35% (range 15–90%) at 12 months (36). A series of 43 hepatocellular carcinomas treated with RF showed a decrease in the immediate postablation scar volume of 21% at 1 month, 50% at 4 months, 65% at 7 months, and 89% at 16 months. This slow decrease in the scar volume has also been reported after cryotherapy (30). Ethanol-induced necrosis seems to decrease in size more often and faster, with reports of a diminution of size in all treated tumors that attained a mean of 45% at 6 months and 63% at 12 months (37).

World Health Organization (WHO) criteria or Response Evaluation Criteria in Solid Tumors (RECIST) criteria (38,39) cannot be applied to assess response to ablative therapies, at least not early during the posttreatment period. By these criteria, anticancer treatment is based on a decrease in tumor size, which is not really applicable to ablation. Other methods are needed to assess the efficacy of ablative treatment. Today, there is no clear consensus about which imaging techniques are the most appropriate for follow-up after ablation and various imaging techniques are used from one study to another. However, the criteria most commonly used to assess this efficacy on CT, MR, or US imaging is the absence of tissue enhancement, probably while awaiting functional imaging (positron emission tomography [PET] scanning).

Liver

Enhanced CT and MR imaging are at present considered the most useful modalities to assess thermal ablation efficacy in the liver. Preliminary reports suggest that the size of the nonenhancing region after RF visualized at CT and MR imaging corresponded to within 2 mm of the size of the necrosis measured histologically (40–42) or with cryotherapy (43).

When RF therapy is successful, a hypoattenuating well-demarcated, round or oval scar is depicted on CT. Areas of higher attenuation can be found within the thermally ablated area after RF, microwave, laser, or cryotherapy, corresponding to hemorrhage. The thermally ablated area does not enhance after injection of contrast medium.

Two particular postthermoablation imaging patterns must be underscored. The first is the presence of wedge-shaped areas of contrast enhancement abutting on the RF scar seen in 12% of patients in the arterial phase on CT (Fig. 9.7) (36). These wedge-shaped areas of contrast enhancement are probably due to perfusion disorders, such as small-vessel thrombosis and arterioportal fistulas induced by ablation. The second pattern found after any type of ablation is a thin peripheral rim of enhancement, usually measuring less than 2 mm in width, which is often seen surrounding the radiofrequency scars (Fig. 9.8). This rim is due to inflammatory and granulation tissue with profuse neovascularization found after most ablative techniques, as that described in an experimental model after focused US (44) or cryotherapy (43), as well as in clinical practice after RF (36,40,45). This rim has been described less commonly in hepatocellular carcinoma treated with alcohol injection (46,47) and in hepatic metastases treated with laser-induced thermotherapy (48,49). The inflammatory rim decreases with time. We found this rim in 24% and 18% of RF-treated tumors, respectively, on MR and CT at 2 months, in 4% on MR at 4 months, and in 2% on MR at 9 months (36). Others have reported this rim in 89% of CT studies after RF treatment within 1 month, in 56% between 1 and 3 months, and in 22% between 3 to 6 months (45).

Residual active tumor foci depicted on CT usually are found at the periphery of the RF-induced lesion, and can appear as a nodule or

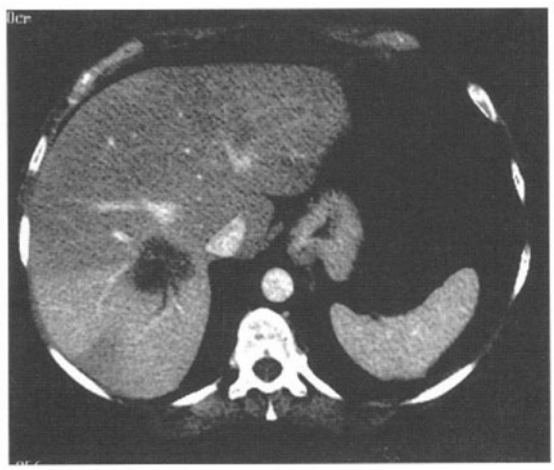

FIGURE 9.7. Two months after RF ablation of a breast cancer metastasis, the scar is not enhanced. There is a large wedge-shaped perfusion disorder demonstrating early and heavy enhancement of the parenchyma in segment VII. Note the faint dilation of the biliary tract at the periphery of the scar, imaged as periportal hypoattenuatting linear structures.

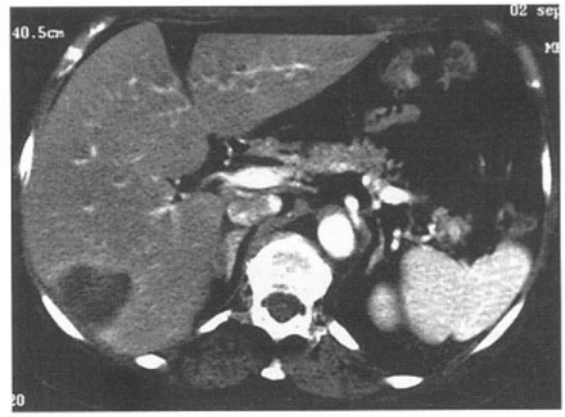

FIGURE 9.8. A CT scan 2 months after RF ablation of a subcaspsular metastasis shows a thin peripheral rim of enhancement corresponding to inflammatory tissue.

local thickening of the peripheral rim. More rarely, an increase in the size of the treated area signifies incomplete treatment. This increase in size, also called the halo pattern of recurrence, is found more frequently in recurrent metastases than with HCC (50).

Foci of active tumor exhibit hypo- or hyperattenuation on CT, and HCC's usually demonstrate contrast enhancement during the arterial phase. In contrast, metastases remain mostly hypovascular, and sometimes demonstrate low-grade enhancement at their periphery on imaging of the portal phase. The arterial phase image is therefore best to detect recurrent HCC, while the portal phase image is best to depict recurrent colorectal metastases. Due to the heat sink effect encountered during thermal ablation with RF, considerable attention should be paid to scars located in the vicinity of large vessels where incomplete treatment is seen more frequently (42,51).

A major question is when postablation imaging follow-up should be initiated and how regularly it should be repeated. It is difficult to appraise results soon after treatment because of the peripheral inflammatory rim that enhances and can be misinterpreted as residual tumor, or small foci of remnant tumor embedded in this rim that may be overlooked. These are reasons why the first imaging studies are usually performed 1 to 3 months after RF, and then repeated every 2 or 3 months. Repeat imaging eventually will demonstrate regrowth of small foci of unablated tumor that remain in the scar, but were too small to be detected earlier. However, for most authors, including Solbiati et al (52), who reported 77% occurring before 6 months, and 96% depicted by 1 year, the likelihood of such local regrowth after 12 months is low (36,53). This signifies that after 1 year, the main aim of follow-up imaging is to search for new hepatic tumors rather than local recurrences.

In most studies, CT and MR are used variably to assess the efficacy of RF treatment. We compared CT and MR in our early experience in RF of liver tumors, imaging every 2 months with both CT and MR (36). Incomplete treatment was depicted in nine cases. At 2 months of follow-up, CT revealed four local failures and MR found eight. However, equivalent imaging results were obtained at 4 months with both imaging techniques, which revealed eight of nine incomplete treatments, with the ninth being discovered at 6 months. T2-weighted images were the most reliable sequences, due to good contrast between the hypointense scar and the mildly hyperintense residual tumor. However, caution should be exercised when distinguishing the mildly hyperintense signal indicative of residual tumor from the heavily hyperintense, fluid-like appearance of liquid necrosis.

Contrast-enhanced harmonic power Doppler US, compared to CT, appears to be useful to demonstrate local relapse after RF treatment. The technique demonstrated a sensitivity of 90% to 98%, a specificity of 100%, and 98% accuracy, in detecting local recurrence 3 to 7 days after RF ablation of hypervascular HCC's (54,55). However, this technique is much less efficient in detecting residual tumor after treatment of colorectal metastases. Among 75% of tumors that showed enhancement before treatment, only 50% of the post-RF local relapses were seen the day after treatment (52).

Imaging of complications is an important reason for follow-up imaging, and CT has a major role to play in this context. One of the more common complications after ablation therapy is an abscess in the liver after RF (56,57), and to a lesser extent after cryotherapy (58). This complication seems to be much more frequent in patients who have a bilioenteric anastomosis. These abscesses typically have been reported after an interval that ranges from 8 days to 5 months (51,56,57). Clinical symptoms may be mild, so imaging plays a major role in their depiction. They usually appear as a gas-containing mass that has developed in the ablated bed. They usually can be drained under CT guidance. However, small gas bubbles are nearly always imaged during ablation either with hyperthermia or cryotherapy, and they can persist for several days. In our experience with RF ablation, all the ablated areas containing gas after 2 weeks always were aspiration-proven abscesses. However, gas bubbles have been described in the liver several weeks after

cryotherapy without a related infection (30). Biliary tract dilation upstream from an ablated area is common, and found in 8% of follow-up imaging in our hands (Fig. 9.7). This condition was always clinically asymptomatic in our experience, as no tumors were targeted for ablation close to the liver hilum.

Lung

One or 2 days after RF ablation, CT imaging depicts an increase in the size and density of the blurred parenchyma surrounding the treated tumor, compared to that imaged immediately after the ablation procedure (Fig. 9.5). This increase in the size of the ablated lesion varies considerably among patients. It can be up to 5 to 10mm and usually is concentric, but can cover a complete lung segment with a blurred outline, unless the border is sharply defined by the neighboring fissure. A small pleural effusion is nearly always seen during the early post-treatment period. After 1 to 2 months, this large and blurred area of consolidation shrinks, and forms a scar with a sharper border and higher tissue density. This scar usually continues to be slightly larger than the targeted tumor. If the treatment is successful, the scar will continue to shrink, but slower than during the first 2 months, akin to that reported for liver (Fig. 9.5).

Using contrast-enhanced CT to assess the efficacy of lung RF ablation has yet to be evaluated, but probably depends on the type of enhancement of the tumor before treatment. Late complications are rare. Early and midterm complications are mostly pleural effusions and pneumothoraces. Hemorrhage is unusual in the lung parenchyma even though minor hemoptysis is common from 1 to 10 days after the procedure. One case of major hemorrhage has been reported (28), and avoiding major vessels during the puncture may be a way to avert such complications. Finally, sepsis may appear as segmental or lobar consolidation on imaging that represents a pneumonia. In cases of long-lasting fever, CT should be used to search for an abscess at the ablation site that generally appears as a partially air-filled cavity instead of the usual scar tissue.

Bones

Computed tomography imaging after ablation of bone tumors demonstrates late changes. After ablation of an osteoid osteoma, healing of the ablated area usually takes more than 1 year. As a small volume is treated, usually with a bare laser fiber or a single RF needle, no changes are usually found in the bone surrounding the ablated lesion; however, early pain relief (usually in less than a week), is the best sign that therapy has been effective.

In the case of malignant bone tumors, late signs of efficacy are a shrunken ablated lesion and healing of bone destruction. No enhancement in ablated areas signifies the absence of viable tumor, as in other organs. Furthermore, after a few weeks, CT often shows a rim of hyperattenuating bone tissue that outlines the external borders of the ablated area (Fig. 9.4), although the true explanation for this appearance remains obscure. Spontaneous high bone density prohibits the study of rim contrast enhancement with CT. However, on MR, this rim appears as low signal on T1-weighted images, and high signal on T2-weighted images. Enhanced signal occurs after injection of gadolinium. These imaging patterns are similar to those of the inflammatory rim described in the liver after all types of ablative therapy, and therefore confirm the hypothesis that this is the external border of the ablated area.

Kidney

The size and enhancement criteria used to assess treatment efficacy in the liver with CT are also valid for kidney tumors after ablation. However, stranding of the perirenal fat, usually roughly parallel to the ablated area is an additional feature that evolves on sequential follow-up CT scans into a more organized rim of hyperattenuating tissue, seemingly delineating the external borders of the ablated area (Fig. 9.9) (59,60). Wedge-shaped nonenhancing areas in the kidney adjacent to the ablated lesion are seen on more than half of the follow-up CT images performed at 2 months. They are probably due to peripheral renal infarcts after coagulation of small arterial feeding branches. A

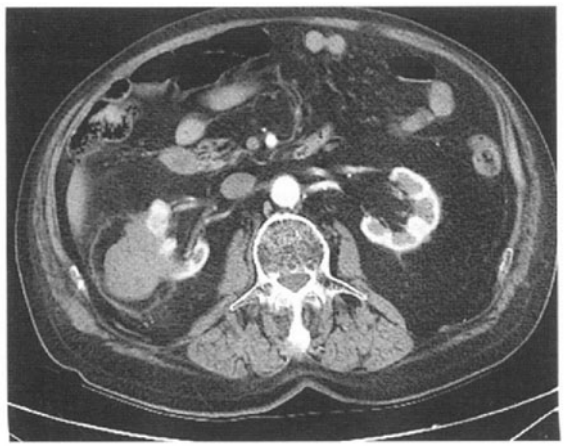

FIGURE 9.9. Follow-up CT scan obtained 8 months after RF ablation of an exophytic renal carcinoma. The unenhanced scar is composed of ablated tumor and a few millimeters of enhanced renal parenchyma adjacent to its inner limit. There is a thin rim of hyperattenuating tissue in the perirenal/peritumorous fat, a few millimeters from the ablated area.

small amount of peri- or pararenal blood is seen in 10% to 40% of ablated renal lesions, but it always disappears on the first follow-up CT at 1 or 2 months (59,60).

References

1. Sheafor DH, Paulson EK, Kliewer MA, DeLong DM, Nelson RC. Comparison of sonographic and CT guidance techniques: does CT fluoroscopy decrease procedure time? AJR 2000;174: 939–942.
2. Kirchner J, Kickuth R, Laufer U, Schilling EM, Adams S, Liermann D. CT fluoroscopy-assisted puncture of thoracic and abdominal masses: a randomized trial. Clin Radiol 2002;57:188–192.
3. Teeuwisse WM, Geleijns J, Broerse JJ, Obermann WR, van Persijn van Meerten EL. Patient and staff dose during CT guided biopsy, drainage and coagulation. Br J Radiol 2001;74: 720–726.
4. Takayasu K, Muramatsu Y, Asai S, Kobayashi T. CT fluoroscopy-assisted needle puncture and ethanol injection for hepatocellular carcinoma: a preliminary study. AJR 1999;173:1219–1224.
5. Kato R, Katada K, Anno H, Suzuki S, Ida Y, Koga S. Radiation dosimetry at CT fluoroscopy: physician's hand dose and development of needle holders. Radiology 1996;201:576–578.
6. Paulson EK, Sheafor DH, Enterline DS, et al. CT fluoroscopy-guided interventional procedures: techniques and radiation dose to radiologists. Radiology 2001;220:161–167.
7. Yueh N, Halvorsen RA Jr, Letourneau JG, Crass JR. Gantry tilt technique for CT-guided biopsy and drainage. J Comput Assist Tomogr 1989;13: 182–184.
8. Kirchner J, Kickuth R, Walz MV, et al. CTF-guided puncture of an unenhanced isodense liver lesion during continuous intravenous injection of contrast medium. Cardiovasc Intervent Radiol 1999;22:528–530.
9. Schweiger GD, Brown BP, Pelsang RE, Dhadha RS, Barloon TJ, Wang G. CT fluoroscopy: technique and utility in guiding biopsies of transiently enhancing hepatic masses. Abdom Imaging 2000;25:81–85.
10. Jacobi V, Thalhammer A, Kirchner J. Value of a laser guidance system for CT interventions: a phantom study. Eur Radiol 1999;9:137–140.
11. Holzknecht N, Helmberger T, Schoepf UJ, et al. [Evaluation of an electromagnetic virtual target system (CT-guide) for CT-guided interventions]. Rofo Fortschr Geb Rontgenstr Neuen Bildgeb Verfahr 2001;173:612–618.
12. Pereles FS, Baker M, Baldwin R, Krupinski E, Unger EC. Accuracy of CT biopsy: laser guidance versus conventional freehand techniques. Acad Radiol 1998;5:766–770.
13. Goodacre BW, Savage C, Zwischenberger JB, Wittich GR, vanSonnenberg E. Salinoma window technique for mediastinal lymph node biopsy. Ann Thorac Surg 2002;74:276–277.
14. Langen HJ, Klose KC, Keulers P, Adam G, Jochims M, Gunther RW. Artificial widening of the mediastinum to gain access for extrapleural biopsy: clinical results. Radiology 1995;196:703–706.
15. Karampekios S, Hatjidakis AA, Drositis J, et al. Artificial paravertebral widening for percutaneous CT-guided adrenal biopsy. J Comput Assist Tomogr 1998;22:308–310.
16. Shah H, Harris VJ, Konig CW, et al. Saline injection into the perirectal space to assist transgluteal drainage of deep pelvic abscesses. J Vasc Interv Radiol 1997;8:119–121.
17. Shibata T, Iimuro Y, Yamamoto Y, et al. CT-guided transthoracic percutaneous ethanol injection for hepatocellular carcinoma not detectable with US. Radiology 2002;223:115–120.
18. Elias D, de Baere T, Goharin A, Lasser P, Roche A. Transpleurodiaphragmatic radiofrequency thermoablation of a liver metastasis. J Am Coll Surg 2000;191:683–685.

19. Antoch G, Kuehl H, Vogt F, Debatin J, Stattaus J. Value of CT volume imaging for optimal placement of radiofrequency ablation probes in liver lesions. J Vasc Interv Radiol 2002;13:1155–1161.
20. Dodd GD III, Frank MS, Aribandi M, Chopra S, Chintapalli KN. Radiofrequency thermal ablation: computer analysis of the size of the thermal injury created by overlapping ablations. AJR 2001;177:777–782.
21. Livraghi T, Goldberg SN, Lazzaroni S, et al. Hepatocellular carcinoma: radio-frequency ablation of medium and large lesions. Radiology 2000;214:761–768.
22. Gangi A, Dietemann JL, Gasser B, et al. Interstitial laser photocoagulation of osteoid osteomas with use of CT guidance. Radiology 1997; 203:843–848.
23. Rosenthal DI. Percutaneous radiofrequency treatment of osteoid osteomas. Semin Musculoskelet Radiol 1997;1:265–272.
24. Rosenthal DI, Hornicek FJ, Wolfe MW, Jennings LC, Gebhardt MC, Mankin HJ. Percutaneous radiofrequency coagulation of osteoid osteoma compared with operative treatment. J Bone Joint Surg [Am] 1998;80:815–821.
25. Callstrom MR, Charboneau JW, Goetz MP, et al. Painful metastases involving bone: feasibility of percutaneous CT- and US-guided radiofrequency ablation. Radiology 2002;224:87–97.
26. Haramati LB, Aviram G. What constitutes effective management of pneumothorax after CT-guided needle biopsy of the lung? Chest 2002; 121:1013–1015.
27. Saji H, Nakamura H, Tsuchida T, et al. The incidence and the risk of pneumothorax and chest tube placement after percutaneous CT-guided lung biopsy: the angle of the needle trajectory is a novel predictor. Chest 2002;121:1521–1526.
28. Vaughn C, Mychaskiw G, II, Sewell P, et al. Massive hemorrhage during radiofrequency ablation of a pulmonary neoplasm. Anesth Analg 2002;94:1149–1151.
29. Cha CH, Lee FT Jr, Gurney JM, et al. CT versus sonography for monitoring radiofrequency ablation in a porcine liver. AJR 2000;175:705–711.
30. McLoughlin RF, Saliken JF, McKinnon G, Wiseman D, Temple W. CT of the liver after cryotherapy of hepatic metastases: imaging findings. AJR 1995;165:329–332.
31. Raman SS, Lu DS, Vodopich DJ, Sayre J, Lassman C. Creation of radiofrequency lesions in a porcine model: correlation with sonography, CT, and histopathology. AJR 2000;175:1253–1258.
32. Crowley JD, Shelton J, Iverson AJ, Burton MP, Dalrymple NC, Bishoff JT. Laparoscopic and computed tomography-guided percutaneous radiofrequency ablation of renal tissue: acute and chronic effects in an animal model. Urology 2001;57:976–980.
33. Hamuro M, Kaminou T, Nakamura K, et al. Percutaneous ethanol injection under CT fluoroscopy for hypervascular hepatocellular carcinoma following transcatheter arterial embolization. Hepatogastroenterology 2002;49: 752–757.
34. Ueda K, Ohkawara T, Minami M, et al. [Non-real-time computed tomography-guided percutaneous ethanol injection therapy for hepatocellular carcinoma undetectable by ultrasonography]. Gan To Kagaku Ryoho 1998;25: 1254–1258.
35. Farres M, de Baere T, Lagrange C, et al. Percutaneous mitoxantrone injection for primary and secondary liver tumors: preliminary results. Cardiovasc Intervent Radiol 1998;21:399–403.
36. Dromain C, de Baere T, Elias D, et al. Hepatic tumors treated with percutaneous radiofrequency ablation: CT and MR imaging follow-up. Radiology 2002;223:255–262.
37. Ebara M, Kita K, Sigiura YM, et al. Therapeutic effect of percutaneous ethanol injection on small hepatocellular carcinoma: evaluation with CT. Radiology 1995;195:371–377.
38. Miller AB, Hoogstraten B, Staquet M, Winkler A. Reporting results of cancer treatment. Cancer 1981;47:207–214.
39. Padhani AR, Ollivier L, Shibata T, et al. The RECIST (Response Evaluation Criteria in Solid Tumors) criteria: implications for diagnostic radiologists. Br J Radiol 2001;74:983–986.
40. Goldberg SN, Gazelle GS, Compton CC, Mueller PR, Tanabe KK. Treatment of intrahepatic malignancy with radiofrequency ablation: radiologic-pathologic correlation. Cancer 2000;88: 2452–2463.
41. Morimoto M, Sugimori K, Shirato K, et al. Treatment of hepatocellular carcinoma with radiofrequency ablation: radiologic-histologic correlation during follow-up periods. Hepatology 2002;35:1467–1475.
42. Solbiati L, Livraghi T, Goldberg SN, et al. Percutaneous radio-frequency ablation of hepatic metastases from colorectal cancer: long-term results in 117 patients. Radiology 2001;221: 159–166.
43. Kuszyk BS, Boitnott JK, Choti MA, et al. Local tumor recurrence following hepatic cryoablation: radiologic-histopathologic correlation in a rabbit model. Radiology 2000;217:477–486.

44. Rowland I, Rivens I, Chen L, et al. MRI study of hepatic tumours following high intensity focused ultrasound. Br J Radiol 1997;70:144–153.
45. Tsuda M, Majima K, Yamada T, Saitou H, Ishibashi T, Takahashi S. Hepatocellular carcinoma after radiofrequency ablation therapy: dynamic CT evaluation of treatment. Clin Imaging 2001;25:409–415.
46. Ito K, Honjo K, Fujita T, Awaya H, Matsumoto T, Matsunaga N. Enhanced MR imaging of the liver after ethanol treatment of hepatocellular carcinoma: evaluation of areas of hyperperfusion adjacent to the tumor. AJR 1995;164:1413–1417.
47. Sironi S, De Cobelli F, Livraghi T, et al. Small hepatocellular carcinoma treated with percutaneous ethanol injection: unenhanced and gadolinium-enhanced MR imaging follow-up. Radiology 1994;192:407–412.
48. Amin Z, Donald JJ, Masters A, et al. Hepatic metastases: interstitial laser photocoagulation with real-time US monitoring and dynamic evaluation of treatment. Radiology 1993;187:339–347.
49. Vogl T, Muller P, Hammersting R, et al. Malignant liver tumors treated with MR imaging-guided laser-induced technique: technique and prospective results. Radiology 1995;196:257–265.
50. Chopra S, Dodd GD III, Chintapalli KN, Leyendecker JR, Karahan OI, Rhim H. Tumor recurrence after radiofrequency thermal ablation of hepatic tumors: spectrum of findings on dual-phase contrast-enhanced CT. AJR 2001; 177:381–387.
51. de Baere T, Elias D, Dromain C, et al. Radiofrequency ablation of 100 hepatic metastases with a mean follow-up of more than 1 year. AJR 2000;175:1619–1625.
52. Solbiati L, Goldberg S, Ierace T, Dellanoce M, Livraghi T, Gazelle S. Radio-frequency ablation of hepatic metastases: post procedural assessment with US microbubble contrast agent—early experience. Radiology 1999;211:643–649.
53. Curley SA, Izzo F, Ellis LM, Vauthey JN, Vallone P. Radiofrequency ablation of hepatocellular cancer in 110 patients with cirrhosis. Ann Surg 2000;232:381–391.
54. Cioni D, Lencioni R, Rossi S, et al. Radiofrequency thermal ablation of hepatocellular carcinoma: using contrast-enhanced harmonic power Doppler sonography to assess treatment outcome. AJR 2001;177:783–788.
55. Meloni MF, Goldberg SN, Livraghi T, et al. Hepatocellular carcinoma treated with radiofrequency ablation: comparison of pulse inversion contrast-enhanced harmonic sonography, contrast-enhanced power Doppler sonography, and helical CT. AJR 2001;177:375–380.
56. Wood TF, Rose DM, Chung M, Allegra DP, Foshag LJ, Bilchik AJ. Radiofrequency ablation of 231 unresectable hepatic tumors: indications, limitations, and complications. Ann Surg Oncol 2000;7:593–600.
57. Zagoria RJ, Chen MY, Shen P, Levine EA. Complications from radiofrequency ablation of liver metastases. Am Surg 2002;68:204–209.
58. Bilchik AJ, Wood TF, Allegra D, et al. Cryosurgical ablation and radiofrequency ablation for unresectable hepatic malignant neoplasms: a proposed algorithm. Arch Surg 2000;135:657–662; discussion 662–664.
59. de Baere T, Kuoch V, Smayra T, et al. Radiofrequency ablation of renal cell carcinoma: preliminary experience. J Urol 2002;167:1961–1964.
60. Gervais D, O'Neill M, Arellano R, McGovern R, McDougal W, Mueller P. Peritumoral CT changes associated with radiofrequency ablation of focal renal lesions: description, incidence, and significance (abst.). Radiology 2001;221(P): 180.